Final Report (2006)

(AFOSR FA5209-06-0184 AOARD)

Title

Nanostructured Sublayers for Improved Light Extraction of Top-emitting and Transparent Organic Electroluminescent Devices

Principal Investigator

Byung Doo Chin, Ph.D.

bdchin@kist.re.kr
Tel +82-2-958-5330

2007. 5.

Korea Institute of Science and Technology (KIST)

Report Documentation Page

1. REPORT DATE **17 MAY 2007**	2. REPORT TYPE **FInal**	3. DATES COVERED **08-05-2006 to 14-05-2007**

4. TITLE AND SUBTITLE **Nanostructured Sublayers for Improved Light Extraction of Top-emitting and Transparent Organic Electroluminescent**		5a. CONTRACT NUMBER **FA520906P0184**
		5b. GRANT NUMBER
		5c. PROGRAM ELEMENT NUMBER
6. AUTHOR(S) **Byung Doo Chin**		5d. PROJECT NUMBER
		5e. TASK NUMBER
		5f. WORK UNIT NUMBER

7. PERFORMING ORGANIZATION NAME(S) AND ADDRESS(ES) **Korea Institute of Science and Technology,39-1 Haweolgok-dong, Sungbuk-ku,Seoul Korea (South),KR,130-650**	8. PERFORMING ORGANIZATION REPORT NUMBER **; AOARD-064021**

9. SPONSORING/MONITORING AGENCY NAME(S) AND ADDRESS(ES) **AOARD, UNIT 45002, APO, AP, 96337-5002**	10. SPONSOR/MONITOR'S ACRONYM(S) **AOARD**
	11. SPONSOR/MONITOR'S REPORT NUMBER(S) **AOARD-064021**

12. DISTRIBUTION/AVAILABILITY STATEMENT
Approved for public release; distribution unlimited

13. SUPPLEMENTARY NOTES

14. ABSTRACT
The work focused on developing flat-panel transparent display using organic light emitting diode. Microstructure Bragg mirrors were also implemented for higher external luminous efficiency and wider color gamut. In addition, organic phosphorescent light emitting materials and devices were studied.

15. SUBJECT TERMS

16. SECURITY CLASSIFICATION OF:			17. LIMITATION OF ABSTRACT	18. NUMBER OF PAGES	19a. NAME OF RESPONSIBLE PERSON
a. REPORT **unclassified**	b. ABSTRACT **unclassified**	c. THIS PAGE **unclassified**	**Same as Report (SAR)**	**28**	

Contents

List of Figures and Tables

Figure 1. Schematics of the bottom and top emission OLEDs and its application area.

Figure 2. Examples of enhanced OLED properties by use of various optical out-coupling methods

Figure 3. (a) Schematic diagram of the laser transfer patterning process used in the fabrication of top-emitting red, green, and blue OLEDs with various light emitting and hole transport layer thicknesses. (b) The layered structures of the top-emitting red, green, and blue devices. (c) The materials used as hole transport layers, light emitting hosts, and dopants.

Figure 4. Transmittance of Mg:Ag composite translucent cathodes with conductivity applicable for devices (10nm and 15nm thickness with Mg:Ag 10:1 ratio)

Figure 5. Experimental apparatus for OLED device fabrication and characterization

Figure 6. FIB-SEM images of conventional and planarized bottom-emitting light emitting OLED pixels: (a) organic layers of small molecular hole transport (α-NPB), and electron transport (Alq_3) materials between ITO and aluminum electrodes; (b) organic layers of PEDOT:PSS/polymeric hole transport/small molecular hole transport materials between the electrodes. Due to insufficient smoothing of the vacuum-deposited small molecular layers, a defect can be observed at the pixel edge (see inside the red circle in (a)).

Figure 7. EL properties of green top-emitting devices with various HTL and EML thicknesses: (a) luminous efficiency versus brightness; (b) EL emission spectrum. The device structure is Al/ITO/PEDOT:PSS (50 nm)/BFEC (20 nm)/α-NPB/CBP:Ir(ppy)$_3$/Balq (5 nm)/Alq$_3$ (35 nm)/LiF/Mg:Ag

Figure 8. (a) 3D contour plot of normalized light as a function of total HTL and ETL thickness, with experimental data points; (b) EL emission spectra of red top-emitting devices with various HTL and EML thicknesses. The device structure is Al/ITO/PEDOT:PSS (80 nm)/BFEC (20

nm)/α-NPB/CBP:Ir(piq)$_3$/Balq (5 nm)/Alq$_3$ (35 nm)/LiF/Mg:Ag. The device codes for each α-NPB/CBP:Ir(piq)$_3$ layer thickness are given in Table 2.

Figure 9. Efficiency-brightness relationship, color emission spectra of top emitting microcavity-OLEDs, and evaluated performance table in the present work

Figure 10. Methods to attach PDMS-based microlens on the external surface of white OLEDs. Increased light intensity of factors 1.1 ~ 1.3 with identical emission spectrum was obtained in case of bottom-emission white OLED.

Figure 11 (a) Design of non-periodic microcavity structure (b) transmittance of dielectric mirror with structure of TiO$_2$ 54nm /SiO$_2$ 90nm /TiO$_2$ 54nm /Glass

Figure 12. Light emitting spectra of green microcavity-enhanced OLED in comparison to the conventional bottom emission OLED (a) CIE 1931 coordinates of RGB (b) which is simulated at various condition.

Figure 13. Application of nanostructures for microcavity-enhancing : on the top emission, flexible, or transparent active matrix OLEDs (*Courtesy of USDC/Samsung SDI*)

Figure 14. Example of angular dependence of microcavity-enhanced OLEDs

Figure 15. Example of nano (sub-micro) imprinting patterns for substrate/electrode modification of OLEDs

Figure 16. Nanopatterns (imprinted) combined with microcavity design

Figure 17. Time of flight (TOF) for measurement of charge carrier mobility

Table 1.   Electroluminescence properties of blue top-emitting OLED devices with various HTLs. The EMLs were 20 nm thick spiro-DPVBi. The small molecular HTL and EML double layers were patterned by using laser transfer.

Table 2. Electroluminescence properties of red top-emitting OLEDs with various hybrid HTL and EML thicknesses. 80 nm PEDOT:PSS was used in all the red devices, so the thickness of the polymeric HTLs on the receptor substrate was 100 nm.

Table 3. Effect of microcavity nanoscale layers on red OLED properties

Abstract

The design and preparation of transparent (emission to both side) or top-emitting organic light emitting devices (OLED) is important since they can be applicable for variety of advanced display applications such as thin, light-weight wearable glass and transparent screen. One of the unique application of transparent OLED for military might be transparent display unit at space-aircraft, which requires operation at low-pressure where conventional LCD will have a reduced response. The use of a top-emitting OLED configuration is an approach to overcoming the existing restrictions of the design of high-resolution active matrix OLEDs.

In order to develop the high performance transparent and top-emitting OLED, fundamental physics and optical analysis on nano-optoelectronic materials for enhanced light extraction of OLED is of great importance although there are many industrial researches and investments.
In this project, we have conducted a basic research on the nano-scale thickness of organic layers optimized for microcavity-enhanced top emission OLED, since the improvement of emission spectra and luminous efficiencies of top-emitting OLEDs are strongly dependent upon the overlapping of optical wavelength for RGB colors and required charge carrier transport path. Combined with recent progress of organic phosphorescent light emitting materials and devices, current research on OLED structures with nanostructured Bragg mirrors provided an improved external luminous efficiency and wide color gamut, which will be an essential part of future flat-panel transparent display.

In a part of top emitting OLED design, stable hole transport layers that effectively smooth the substrate were demonstrated. Double-layer transfer with laser thermal patterning was used to simplify the fabrication of hole transport layers with various thicknesses, with the aim of optimizing the cavity effect in the top-emitting devices. By carrying out optical simulations and experiments, the optimal thicknesses of the hole transport layers for blue, green, and red devices were established. In the section for micro-lens array, fabricated lens that could enhance the external light extraction by a factor of 1.3 were applied for state-of-the-art white OLED devices. Finally, fundamental design of non-periodic Bragg reflector was applied for high-performance microcavity OLED (aimed for bottom, top, and transparent emission). Results showed that simulated spectrum intensity of microcavity OLED using TiO_2 and SiO_2 multilayer increased more than 30 % compared to the conventional OLED. Also, microcavity OLED with CIE coordinates of various angle not seriously changed. Green and Blue device showed improved color coordinate. Based on these simulated data, experimental design of microcavity OLED device will be performed and evaluated using the highly efficient phosphorescent OLED materials.

Based on the investigated fundamental opto-electronic device properties of OLED which is aided by nano-scale thin film structure, we will conduct the research and development of high performance top emitting and transparent OLED with unique nanostructures, which will be innovative OLED design both for nano-optoelectronic device technology and organic electronic device physics.

I. Goal of Research

- Nano/microstructured layers (Microcavity Effects) for top-emission and transparent OLED mode : for Improved light extraction efficiency of OLED
- Efficiency up to 30% increase over conventional OLED, with improved CIE1931 colour coordinates (x,y)
> Red 6Cd/A, (0.67, 0.33)
> Green 35Cd/A, (0.30, 0.60)
> Blue 3Cd/A (0.15, 0.10)
- Evaluation and characterization of optical and electrical properties of OLED (state-of-the-art phosphorescent red, green blue)

II. Annual Scope of Activities

Target/Activity	Results	% of achievement (1st year)	% of achievement (as final)
Bottom emission OLED properties	- Red 6.0 cd/A, (0.67, 0.32) - Green 35 cd/A, (0.33, 0.60) - Blue 5.0 cd/A (015, 0.15)	100%	100%
Top emission OLED properties	- Red 5.5 cd/A, (0.69, 0.31) - Green 24 cd/A, (0.23, 0.72) - Blue 1.8 cd/A (015, 0.07)	100%	80%
Development of Nanostructured layers for planar microcavity effects	-Design and Fabrication of Dielectric Bragg Mirror ($TiO_2/SiO_2/TiO_2$) - Microlens array fabrication	80%	60%
Design and simulation of optical properties of OLED	- Simulation of Microcavity Effects for Efficiency Boost-up	80%	76%
	Overall	(92)%	(76)%

III. Background, Motivation, and Necessities of Research

The growth in the information technology market in recent years has resulted in an increased demand for technologies on high-performance devices that are lightweight, thin and power-efficient. Organic light emitting diode (OLED) displays enable the production of advanced electronic devices, such as transparent, flexible, and ultra-thin displays [1-2]. The backplane design of active matrix OLEDs with uniform drive current output can be achieved through the use of low-temperature polysilicon thin film transistors (TFTs) and a uniformity compensation scheme for both pixel and driver circuitry [3]. However, a highly integrated backplane with more than three or four TFTs within each pixel is required for the fabrication of a high-performance polysilicon TFT backplane, which results in a decreased aperture ratio for a conventional bottom-emitting OLED design. The use of a top-emitting OLED configuration is one approach to overcoming such restrictions on the design of active matrix OLEDs; this configuration reduces the required luminance level by enhancing the aperture ratio and provides improved external emission efficiency and color purity because of microcavity effects [4-6].

Top emission OLEDs can be fabricated on opaque substrates, such as silicon or flexible metal foil [7], but usually require the planarization of the substrate backplane. The development of a highly reflective anode with the appropriate work function and a transparent cathode with enhanced conductivity are further technological challenges for the production of efficient top-emitting OLEDs [8-10]. Moreover, the emission spectra and luminous efficiencies of top-emitting OLEDs are strongly dependent upon the thicknesses of the organic layers and the injection properties of the reflective anode. Wu *et al.* [11] analyzed the outcoupling efficiency, color shift, and Lambertian offset of top-emitting OLEDs as a function of organic layer thickness, which consistent with the general resonance effect for ideal cavity, showing the trade-off in efficiency and Lambertian offset. According to recent experimental and simulation data, top-emitting OLEDs can be more efficient and have better color purity than conventional bottom-emitting OLEDs, at least in a direction perpendicular to the substrate [12-13]. Figure 1 illustrates the schematic features of the bottom and top emission OLEDs and its characteristics.

Meanwhile, if both anode and cathode are transparent metals (transparent OLED), it may be used for future architectural, automotive, wearable electronic applications based on its features that include thin, lightweight form and transparency. However, due to the combination of metal/organic interfaces and optical resonance effect, there exist some technological challenges for improving top-emitting and transparent OLED's performance to a level of conventional bottom emission type. Optical design of OLED has received a great deal of attention as a means of tailoring its emission properties, since almost 80% of the generated light of OLED is lost due to wave-guiding and total internal reflection in the glass substrates (Figure

2). Recently, various submicro- and nano-patterned (or layered) structures are applied to enhance the light extraction efficiency. Two dimensional photonic crystals enhance the out-coupling of light along the surface normal, as well as use of reflecting surfaces or distributed Bragg reflectors. [14-16]. It has been also found that the external quantum efficiency and also the spectral characteristic significantly depend on the OLED architecture, in particular on the layer thicknesses, as a consequence of optical interference effects [17-18]. Consequently, many efforts have been performed in order to improve the light out-coupling efficiency of OLED, for example, use of ordered microlens arrays [19]. Another references and specific application results of various out-coupling schemes for OLED are given in Figure 2.
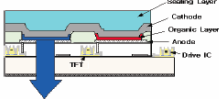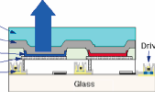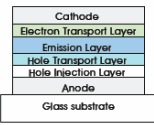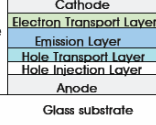
	Bottom-emitting OLED	Top-emitting OLED
Emission direction	**Emission to TFT side**	**Emission to transparent cathode side**
Structure	**Transparent anode** **Reflective cathode**	**Reflective anode** **Semi-transparent cathode**
Character istics	Simple structure and process Low aperture ratio(<40%) Short lifetime and low resolution	Complicated structure and manufacturing High aperture ratio(40~70%) Long lifetime and high resolution Wide color gamut

Figure 1. Schematics of the bottom and top emission OLEDs and its application area.
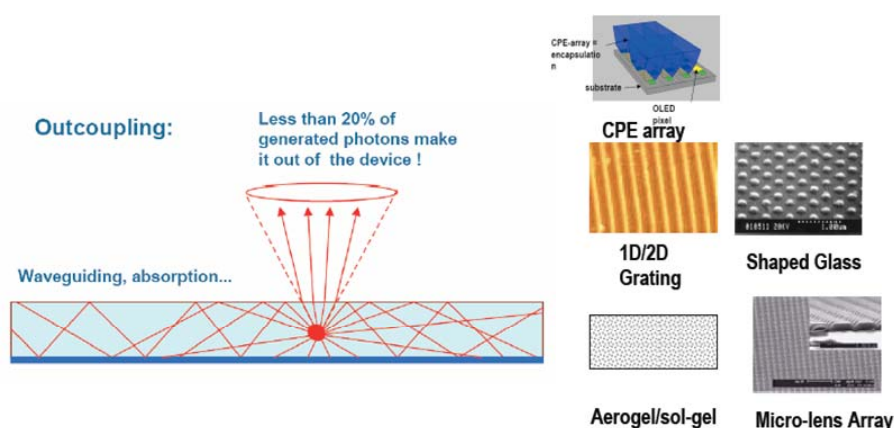
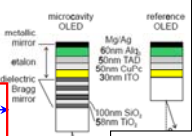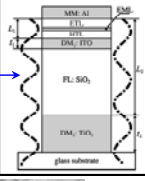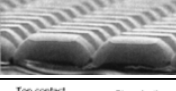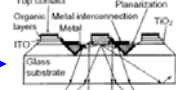| Schemes	Features	Factor (conventional=1.0)	Ref.
Conventional Dielectric Mirror		1.5 ~ 5 (for individual colors)	Tokito *et al.*, J.Appl.Phys. 86, 2407 (1999)
Multi-wavelength Resonance Cavity		1.3	Shiga *et al.*, J.Appl.Phys. 93. 19 (2003)
Top Emission		1.0 ~1.2	Kanno *et al.* Appl. Phys. Lett. 86, 263502 (2005)
Microlens		~1.5	Möller et al. J.Appl.Phys. 91, 3324 (2002)
Patterned/shaped Substrates		~1.9	Garbuzov et al. Opt. Lett. 22, 396 (1997)

Figure 2. Examples of enhanced OLED properties by use of various optical out-coupling methods

In the project during the 1st year, we have employed the novel, polymeric materials that can effectively planarize the substrates for OLED devices. The use of a layered coverage on the receptor enables the stable fabrication of light emitting pixels for both bottom- and top-emitting OLEDs. The laser thermal patterning was used to fabricate RGB top-emitting OLEDs. This effective solid-to-solid transfer process can simplify the OLED layer patterning, which simultaneously transfer many organic layers onto the receptor. Using this method, we could easily obtain the **nanoscale organic thickness differently optimized for each pixels of RGB colors**, which can significantly enhance the color purity as a result of the optimized cavity effect.

Another approach for improving light out-coupling efficiency of top-emission and transparent-type OLED device is a development and application of **nanostructured sublayers,** which can be applied for top emission, transparent, and illumination-type next generation OLEDs. For a specific application for red, green, and blue-emitting OLED, we have designed **microcavity OLED by distributed Bragg reflector model** (DBR). Simulated results show that spectrum intensity of microcavity OLED using TiO_2 **and** SiO_2 **multilayer increased more than 30 % compared to the conventional OLED.** Also, microcavity OLED with CIE1931 coordinates of various angle not seriously changed. Green and Blue device showed further improved color coordinate. Possible optical nanostructures using the method of nano-imprinting with soft lithography, which will fabricate photonic crystal structure of high-refractive-index materials for improved light extraction, are also under way of design for 2nd year activities.

IV. Methods for Research Activities

1. Fabrication of Top-Emitting OLED with Microcavity Effects

- Basic OLED structures for transparent and top-emitting cathodes

　With transparent anode (ITO) and translucent cathode: **transparent OLED**

　　Basic structures :

　　　ITO/PEDOT:PSS/BFEC interlayer/Light emitting materials (EML, RGB)
　　　　/BCP/Alq$_3$/Mg:Ag

　With reflective anode (Aluminum) and translucent cathode: top-emission OLED

　　Basic structures :

　　　Al/ITO/PEDOT:PSS/BFEC interlayer/Light emitting materials (EML, RGB)
　　　　/BCP/Alq$_3$/Mg:Ag

- Materials & Device preparation : A reflective anode consisting of an aluminum (200 nm thick) layer topped with 12.5 nm of indium tin-oxide (ITO) was fabricated. Each light emitting pixel (2 mm × 2 mm) was patterned with an insulator (using a commercial photoresist) so that stripe patterns (80 μm width and 142 μm pitch) were achieved. The substrates were cleaned with ultra-sonication in deionized water and isopropyl alcohol. They were rinsed again in a chamber filled with hot isopropyl alcohol vapor and then subjected to UV-O$_3$ treatment for 15 minutes. PEDOT:PSS (50 nm Baytron P TP AI4083 or 80 nm CH 8000, *Bayer AG,* with 0.45 μm PTFE filtering) was spin-coated onto each substrate, followed by drying at 150℃ for 10 minutes. Poly(9,9'-dioctylfluorene-co-bis-N,N'-(4-ethoxycarbonylphenyl)-bis-N,N'-phenyl-benzidine (BFEC) was spin-coated from a 0.8 wt% solution in anhydrous toluene and employed as a polymeric hole transport layer (20 nm). These substrates were used as receptors of laser transfer patterning after annealing at 200℃ for 10 minutes in air. For the laser transfer patterning process, stacked EML/HTL bi-layers were vacuum-coated onto the transfer film and transferred to the substrate. A small molecular HTL, N,N'-diphenyl-N,N'-bis(1-naphthyl)-(1,1'-biphenyl)-4,4'-diamine (α-NPB), was used as a supplementary HTL. 4,4'-N,N'-Dicarbazole-biphenyl (CBP) was used as a host EML material for the phosphorescent red- and green-emitting layers. The metal complexes *fac*-tris(1-phenylisoquinoline)iridium (III) [Ir(piq)$_3$] and *fac*-tris(2-phenylpyridine) iridium (III) [Ir(ppy)$_3$] were employed as the red and green emitting dopants respectively, with concentrations in CBP of 12% for Ir(piq)$_3$ and 7% for Ir(ppy)$_3$. 2,2',7,7'-tetrakis-(2,2'-Diphenyl-vinyl)-spiro-9,9'-bifluorene (spiro-DPVBi) was used as the blue-emitting fluorescent material. The transport of material from the donor to the receptor is carried out while the donor and receptor are held in intimate contact [16]. After the laser transfer

process that provides precise color patterning, a 5 nm thick hole-blocking layer (aluminum(III)bis(2-methyl-8-quinolinato)4-phenylphenolate, Balq) was deposited, followed by the evaporation of a 35 nm tris(8-hydroxyquinoline)-aluminum (Alq$_3$) electron transport layer. Thin lithium fluoride and magnesium-silver alloy were thermally evaporated with an evaporation rate ratio of 10:1 to form a translucent cathode (10 nm). The schemes for the color patterning and device fabrication processes as well as the materials employed in this study are shown in Figure 3.
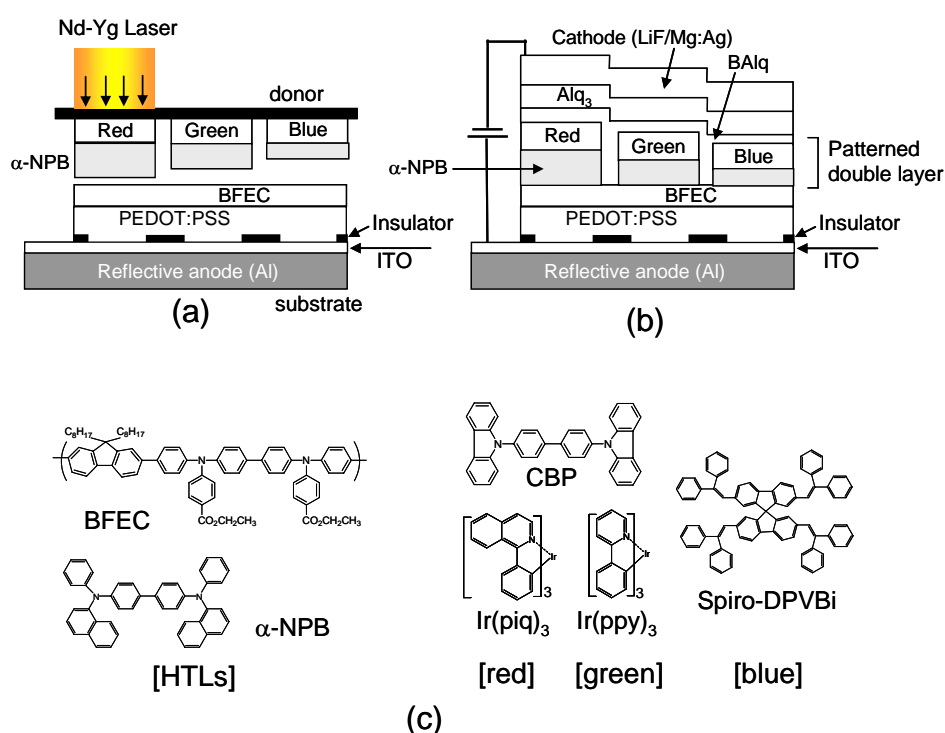
Figure 3. (a) Schematic diagram of the laser transfer patterning process used in the fabrication of top-emitting red, green, and blue OLEDs with various light emitting and hole transport layer thicknesses. (b) The layered structures of the top-emitting red, green, and blue devices. (c) The materials used as hole transport layers, light emitting hosts, and dopants.

2. Fabrication of Translucent (semi-transparent) Cathodes for OLED

- ITO (indium tin oxide) or other doped wide-band-gap oxide materials have good transparency and conductivity, but deposition is only possible with radiofrequency (rf) sputtering process, which cause serious damage on the organic layers under the cathode.

Therefore, it is only used as anode (sputtered on top of glass) and excluded for transparent cathode candidate at this project.

- <u>Mg:Ag</u> deposition is conducted with thermal evaporation, which does not degrade the

organic layers by deposition process (See Figure 4 for transmittance)

We have set the optimized Mg:Ag ratio and thickness : range is co-deposition of Mg:Ag = 10:1, with 10~15nm thickness
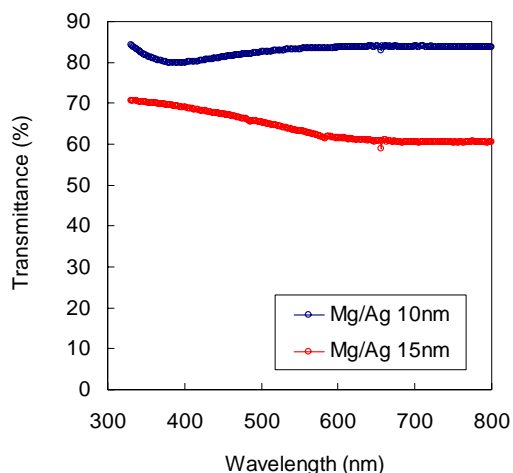
.

Figure 4. Transmittance of Mg:Ag composite translucent cathodes with conductivity applicable for devices (10nm and 15nm thickness with Mg:Ag 10:1 ratio)

- Other Characterization: Thickness of spin-coated organic layers was measured with alpha-step surface profiler P-10 (Tencor). The surface morphology of BFEC film was analyzed by atomic force microscopy (AFM, Nanoscope IIIa, Digital Instruments Co.). The luminescence-voltage (L-V) and current efficiency-voltage characteristics were measured using a Keithley 236 source measurement unit and CS-100 spectrophotometer.

Figure 5. Experimental apparatus for OLED device fabrication and characterization

2. Development of Micro/or Nanostructures for Microcavity OLED

- <u>Photonic crystal (microlens) approach</u> : PDMS microlens with Si/SiO_2 mold
    Application for top-emitting and transparent OLED for microcavity effect, I
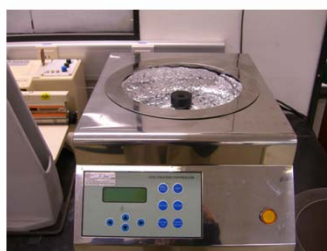 improving light outcoupling efficiency
    Challenges: removing haze, defect, and use of proper interfacial layer
    Contact transfer of nanoparticle-coated layer onto OLED semi-transparent cathode
  (use of interfacial layer, which will improve adhesion between transferred
    nanoparticle composite layer and donor substrate of OLED cathode)

- <u>Dielectric layers</u> for microcavity effect
  Formation of stacked dielectric layers on top of cathode
    SiO_2 : n (refractive index) =1.46
    TiO_2 : n = 2.30
  However, direct rf-sputtering onto organic/cathode surface is not possible due to
  severe sputtering-damage
      --- 1. Insertion of dielectric layers between glass/ITO(transparent anode)
          2. Use of lamination transfer technique : transfer of PDMS/dielectric layers
              Onto semi-transparent cathodes, *etc*.

3. Optimization and Evaluation of Devices
  - Compare basic device performance of transparent & top emission OLED with
  devices employing microcavity layers (*2~3 attempts in section 4 experimental methds*)
  - Evaluation of I(current)-V(voltage)-L(luminance) characteristics and efficiency
  (current, by cd/A unit, and power, by lm/W unit)
  - Evaluation of color coordinate : luminous spectrum and CIE1931(x,y)
  - Find most effective method for microcavity-effect
      Angular dependence of produced light (intensity and color) by microcavity effects

V. Results of 2006 Research, with Technical Discussion

SUMMARY

===

1. Establish Top-Emission OLED Microcavity Structure (~80% of final target)

Obtained Device Properties :

Red (0.69, 0.31, 5Cd/A) Green (0.23,0.72, 24Cd/A), Blue (0.15,0.07, 1.8Cd/A)

2. Microlens-enhanced OLED (White OLED, factor 1.1 ~ 1.3)

3. Design of Non-periodic Microcavity Nanoscale Layers for OLED Application

===

1. Top-Emission OLED Microcavity Structure with Effective Hole Transport Layer Structure, suitable for high-resolution laser patterning

The optimization of the film thicknesses of the organic layers of top-emitting OLEDs to achieve more effective cavity structures requires different charge transport layer thicknesses for the red, green, and blue colors due to their different characteristic optical path lengths [20]. Therefore, the additional fine patterning of the hole/electron transport layers (usually with an ultra-thin shadow mask) or the fabrication of anodes with variable thickness have been used to achieve enhanced color gamut and a higher top emission efficiency [21]. In the present work, the laser transfer patterning of organic materials [22-23] was used in the simultaneous transfer of a hole transport layer (HTL)/emission layer (EML) bi-layer onto a substrate planarized with a hybrid hole transport layer, which effectively reduces the number of shadow mask patterings required in the fabrication of full color/high resolution top-emitting OLEDs.

The remarkable smoothing effect of hybrid, polymeric HTLs (PEDOT:PSS and BFEC) on a light emitting pixel are shown in Figure 6. Figure 6a shows an image of the pixel obtained with scanning electron microscopy combined with a focused ion beam (FIB-SEM), which shows the positional defects that can cause device breakdown due to a short-circuit. The fabrication of stable OLED emitting pixels for a fine-patterned device (as in the active matrix devices) can be aided by the use of the thick HTL buffers introduced in the present study (see inside the red circle in Fig. 6b). Although this image is of a conventional bottom-emitting device, it is also relevant to top-emitting pixels and this smoothing effect is very effective for HTL thicknesses of more than 100 nm.
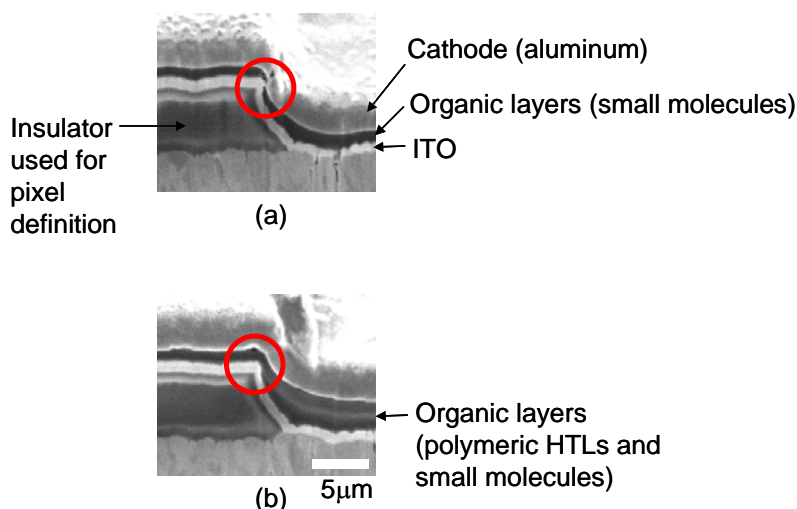
Figure 6. FIB-SEM images of conventional and planarized bottom-emitting light emitting OLED pixels: (a) organic layers of small molecular hole transport (α-NPB), and electron transport (Alq$_3$) materials between ITO and aluminum electrodes; (b) organic layers of PEDOT:PSS/polymeric hole transport/small molecular hole transport materials between the electrodes. Due to insufficient smoothing of the vacuum-deposited small molecular layers, a defect can be observed at the pixel edge (see inside the red circle in (a)).

A brief comparison of the top-emitting OLED devices with 50 nm thick PEDOT:PSS (AI4083)/small molecular HTL and PEDOT:PSS/polymeric/small molecular HTLs (hybrid multi-stack) is given in Table 1, which shows their blue-emitting electroluminescence (EL) properties. The initial selection of the HTL and ETL thicknesses of the top-emitting devices for blue, green and red emission was carried out with optical simulations based on a system consisting of an emitting medium sandwiched between a reflective mirror and a semitransparent cathode, which exhibits the optical microcavity effect [24-26]. All devices exhibit a 460 nm maximum peak with a significantly narrower EL spectrum than bottom-emitting devices using the same blue emitter, resulting in CIE (Commission Internationale de L'Eclairage) 1931 (x,y) color coordinates of (0.13 ~ 0.14, 0.05 ~ 0.06), which is pure blue emission. The brightness and luminous efficiency (measured at 8 V) of devices using the polymeric HTL (devices B2 and B3 with stable edge-cutoff structures, as shown in Fig. 6b) were somewhat lower than those for B1 (small molecular HTL), possibly due to the limited hole transport mobility of the polymeric HTL (BFEC) compared to that of α-NPB. However, these devices with a hybrid HTL still exhibit an acceptable color index with a pure blue light emitting spectrum.

Figure 7 shows the EL properties (efficiencies and light emitting spectra) of the green top-emitting devices prepared with laser patterning; small molecular HTL and green EML

double layers were also transferred onto this substrate coated with 50 nm AI4083 and 20 nm BFEC. The efficiencies are strongly dependent upon the thicknesses of the small molecular HTL (α-NPB) and the EML, with a maximum value of 24 cd/A at 1000 cd/m^2 (reached at 9 V, with a 90 nm HTL and a 30 nm EML). Interestingly, the green emission peaks of these devices were found to be significantly red-shifted when the HTL thickness was increased up to 110 nm (see Fig. 7b), compared to the EL spectra of the 90 nm HTL devices which contain peaks at 524~526 nm. Considering the properties of a conventional bottom emission device with a 30 nm thick CBP:Ir(ppy)$_3$ EML [21] (with a maximum EL peak at 512 nm), this shift in the emission spectrum does not result in a great loss of luminous efficiency but significantly reduces the achievable brightness (see the brightness-efficiency curve in Fig. 7a). Therefore, the optimal total hybrid HTL thickness for the green phosphorescent top-emitting device was found to be 160 nm (PEDOT 50 nm/BFEC 20 nm/α-NPB 90 nm).

Table 1. Electroluminescence properties of blue top-emitting OLED devices with various HTLs. The EMLs were 20 nm thick spiro-DPVBi. The small molecular HTL and EML double layers were patterned by using laser transfer.

Code	HIL (50nm)	*HTL* *(nm)*	Turn-on voltage*(V)* at 1cd/m^2	Brightness *(cd/m^2)* at 8V	Efficiency *(cd/A)* at 8V	CIE1931 *(x,y)*
B1	**AI4083**	**α-NPB** (90)	3.6	450	1.89	(0.13, 0.06)
B2	**AI4083**	**BFEC/α-NPB** (20/70)	3.6	210	1.48	(0.14, 0.05)
B3	**AI4083**	**TFB/α-NPB** (20/70)	3.7	137	1.40	(0.14, 0.05)

Variation of the thicknesses of the organic HTL, EML, and ETL layers affects both the electrical and optical properties of the devices, and the optimization of the thicknesses results in improved emission intensity, at least in the direction perpendicular to the plane of the substrate. While green/blue top emitting devices showed nearly comparable external quantum efficiency with bottom emission, further improvement of quantum efficiency in case of red top emitting device was reported by Huang *et al.* [6]. They have explained such difference by the analysis of decay rate of red, green, and blue triplet excitons. Table 2 shows the results of our investigation of the variation of the light emission characteristics of top-emitting red devices (brightness, efficiency, and color spectrum) with the thicknesses of the organic layers.
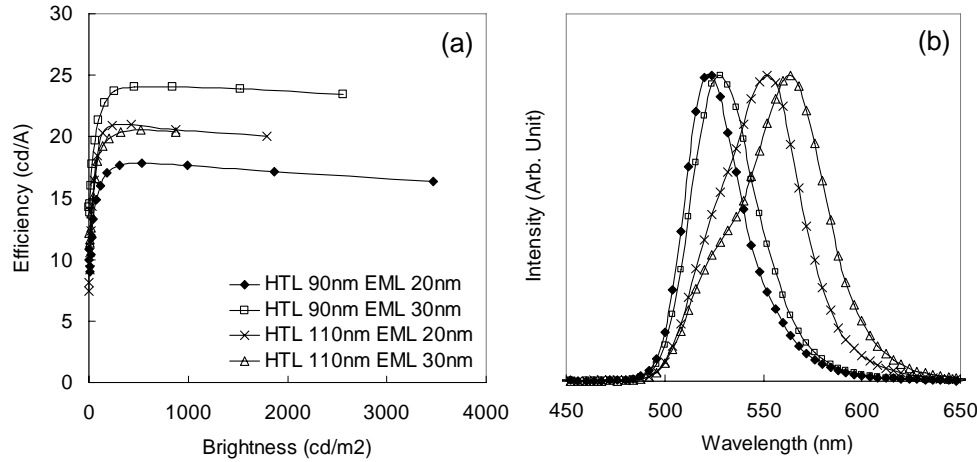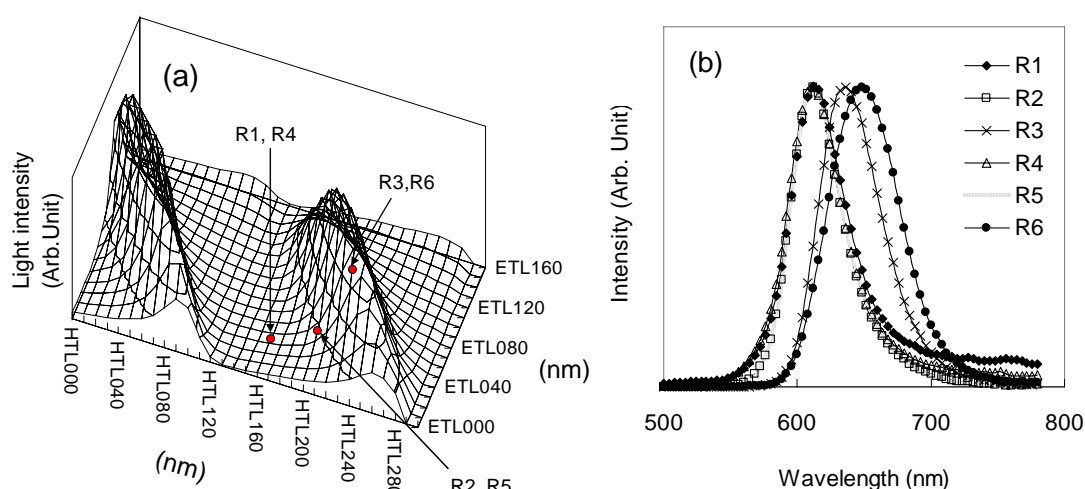
Figure 7. EL properties of green top-emitting devices with various HTL and EML thicknesses: (a) luminous efficiency versus brightness; (b) EL emission spectrum. The device structure is Al/ITO/PEDOT:PSS (50 nm)/BFEC (20 nm)/α-NPB/CBP:Ir(ppy)$_3$/Balq (5 nm)/Alq$_3$ (35 nm)/LiF/Mg:Ag

Table 2. Electroluminescence properties of red top-emitting OLEDs with various hybrid HTL and EML thicknesses. 80 nm PEDOT:PSS was used in all the red devices, so the thickness of the polymeric HTLs on the receptor substrate was 100 nm.

Code	HTL *(nm/nm)* :BFEC/α-NPB	EML *(nm)* :CBP:Ir(piq)$_3$ (12%)	Turn-on voltage*(V)* at 1cd/m^2	Brightness *(cd/m^2)* at 8V	Efficiency *(cd/A)* at 8V	CIE1931 *(x,y)*
R1	20/60	30nm	3.5	71	0.20	(0.63, 0.36)
R2	20/100	35nm	3.4	555	2.19	(0.65, 0.35)
R3	20/130	30nm	3.4	1070	5.05	(0.69, 0.31)
R4	20/60	40nm	3.7	61	0.41	(0.63, 0.37)
R5	20/100	35nm	3.2	412	2.46	(0.65, 0.35)
R6	20/130	40nm	3.4	376	4.19	(0.70, 0.30)

Since the focus of this study was the finding of optimal top-emitting device structure with thick HTLs containing substrate-smoothing polymeric materials, a wide range of HTL thicknesses was considered for total HTL thicknesses of 160 to 230 nm. In Fig. 8a, the normalized light intensity (brightness/required brightness at the corresponding color index, obtained with the classical optical model [24-26]) as a function of total HTL and ETL thickness is shown as a 3D contour plot. The base conditions for these calculations were as follows: 200 nm aluminum/12.5 nm ITO (reflective anode), 10 nm Mg:Ag (semitransparent cathode), and a 5 nm hole blocking layer. The contours of normalized brightness are concentric ellipses with maxima for HTL/ETL thicknesses of 40 nm/60 nm, 220 nm/70 nm and feasible ranges of 30~60

nm/30~70 nm and 210~240 nm/30~70 nm, respectively. Experimental points from Table 2 (R1 ~ R6, with an identical ETL thickness of 35 nm) are also shown in Fig. 8a, and are mostly in accord with the simulated results in terms of light emission properties such as efficiency and brightness. Although higher light emission intensity is expected for HTL/ETL thicknesses of 40 nm / 60nm, the limitations of the electron transport properties of most organic compounds make it difficult to design top-emitting devices with an ETL thickness greater than 40 nm. Therefore, with ETL thickness of 30~40nm, the HTL thickness windows of 65~90 nm and 230~250 nm are the feasible ranges for achieving a positive cavity effect in red devices.


Figure 8. (a) 3D contour plot of normalized light as a function of total HTL and ETL thickness, with experimental data points; (b) EL emission spectra of red top-emitting devices with various HTL and EML thicknesses. The device structure is Al/ITO/PEDOT:PSS (80 nm)/BFEC (20 nm)/ -NPB/CBP:Ir(piq)$_3$/Balq (5 nm)/Alq$_3$ (35 nm)/LiF/Mg:Ag. The device codes for each -NPB/CBP:Ir(piq)$_3$ layer thickness are given in Table 2.

The experimental results for R3 and R6 show the enhancement of the efficiency by the cavity effect; these devices satisfy the conditions for thick HTLs, which are also beneficial for their smoothing effects on the light emitting pixels. However, there seems to be compensation between the resonance wavelength-induced microcavity effect and the limitations on hole/electron transport efficiency, which might result in a drop of brightness. With an α-NPB thickness of 60~100 nm (total HTL thickness 160~200 nm), red top emission has very low efficiency (less than 2.5 cd/A) with a spectrum peak of 612 nm, as can be seen in Fig. 8b. Note that an emitting layer of CBP doped with 12% Ir(piq)$_3$ in a bottom-emitting device structure produces 4.8~5.5 cd/A with CIE 1931 color coordinates of (0.67, 0.33), which corresponds to

peak emission at 624 nm. The blue-shift and lower efficiency of top-emitting devices (R1, R2, R4, and R5) can be explained in terms of the mismatch of the emitting zone within the microcavity structure and its resonance wavelength. More efficient red emission is achieved for a total HTL thickness of 230 nm, with 636 nm peak emission, CIE 1931 coordinates of (0.69, 0.31), and 5.05 cd/A. A further red-shift of the emission peak (centered at 648 nm; 0.70, 0.30) resulted in a trade-off between efficiency and brightness, as can be seen in Table 2 and Fig. 8ab.

Figure 9 summarize the efficiency of top emission microcavity devices developed in the project and improved color spectrum compared to the conventional bottom emission RGB devices. We used polymeric materials such as PEDOT:PSS (hole injection) and BFEC (hole transport) that can effectively planarize the receptor substrates.
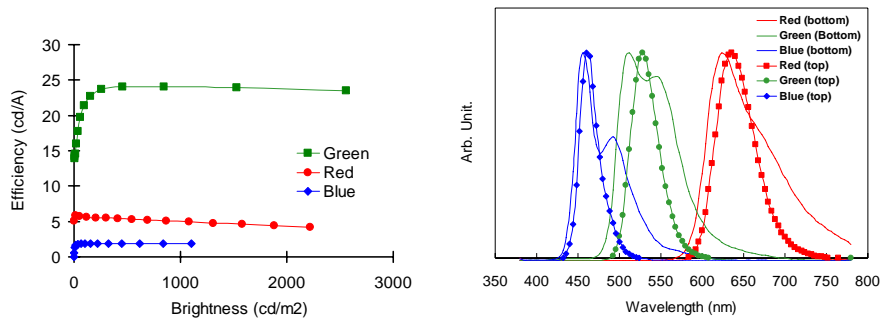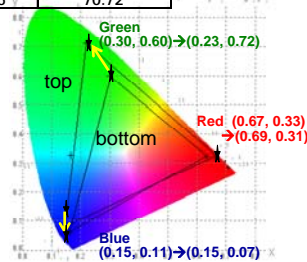

Target (top emission OLED, RGB)

Material	Required Brightness (cd/m²)	Ratio	x	y	Eff. (cd/A)	Current Density (A/m²)
Red	459	0.23	0.67	0.33	6	76.52
Green	1246	0.62	0.3	0.6	35	35.60
Blue	300	0.15	0.15	0.1	3	100.02
White	100	1.00	0.31	0.31	9.5	70.72

Obtained at 1st year (top emission OLED, RGB)
: comparable result in terms of required brightness
  80% of final target

Material	Required Brightness (cd/m²)	Ratio	x	y	Eff. (cd/A)	Current Density (A/m²)
Red	513	0.26	0.69	0.31	5.5	93.19
Green	1280	0.64	0.23	0.72	24	53.34
Blue	213	0.11	0.15	0.07	1.8	118.13
White	100	1.00	0.31	0.31	7.6	88.22

Figure 9. Efficiency-brightness relationship, color emission spectra of top emitting microcavity-OLEDs, and evaluated performance table in the present work

The use of a layered HTL coverage on the receptor enables the stable fabrication of light

emitting pixels for both bottom- and top-emitting OLEDs. This alternative and simplified color patterning method was used to simultaneously transfer HTL/EML double layers onto these receptors, and laser thermal patterning was used to fabricate RGB top-emitting OLEDs with various HTL thicknesses, which can significantly enhance the color purity as a result of the optimized cavity effect. **Optical simulations were performed in order to optimize the thicknesses of the hole transport layers for blue (140 nm), green (160 nm), and red (230 nm) devices, resulting in CIE 1931 coordinates of (0.14, 0.06) at 1.4 cd/A, (0.23, 0.72) at 24 cd/A, and (0.69, 0.31) at 5 cd/A, respectively.**

2. Microlens-enhanced OLED

It is reported that factor of 1.2~1.9 external light extraction intensities can be achievable by using of various outcoupling-enhancement technique, as summarized in Figure 2. We have attached polydimethylsiloxane (PDMS) microlens array onto the glass substrate of bottom-emission WOLED and surface of semi-transparent cathode. Effects of outcoupling enhancement for both WOLED lighting properties was examined. Due to the low refractive index of PDMS microlens, factors of improved light intensity is not great, as seen in Figure 10. Currently, we are working for finding a better high-refractive-index material (polymer with inclusion of inorganic particles), which is suitable for cost-effective microlens-processing such as roll-to-roll hot embossing process.
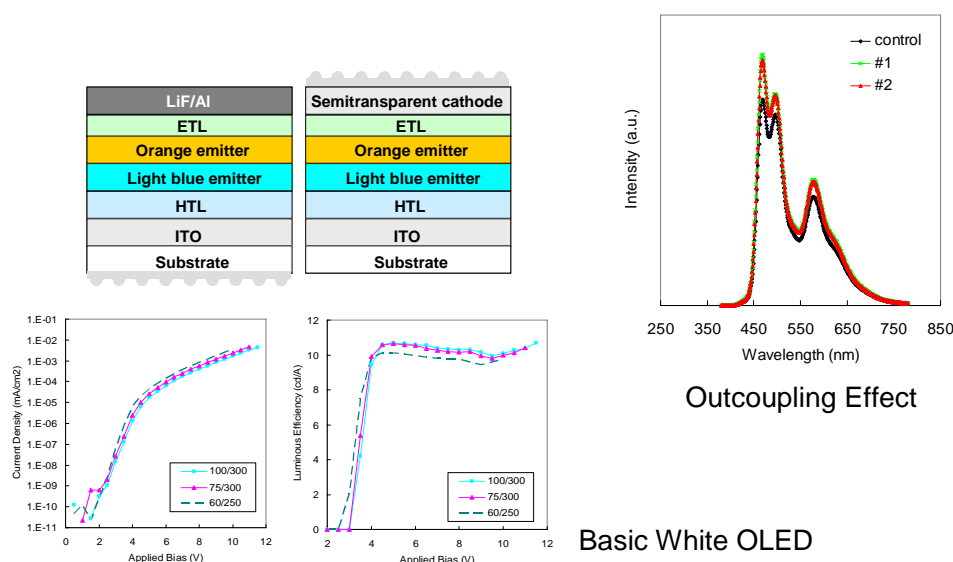

Figure 10. Methods to attach PDMS-based microlens on the external surface of white OLEDs. Increased light intensity of factors 1.1 ~ 1.3 with identical emission spectrum was obtained in case of bottom-emission white OLED.

3. Design of Non-periodic Microcavity Nanoscale Layers for OLED Application

In addition to the significant progress in the device structure of organic multi-layers, optical design of OLED using microstructured array has received a great deal of attention as a means of tailoring its external light emitting properties, since almost 80% of the generated light of OLED is lost due to wave-guiding and total internal reflection in the glass substrates (see Figure 2). It has been found that the external quantum efficiency and the spectral characteristic significantly depend on the OLED architecture, in particular on the layer thicknesses as a consequence of optical interference effects [14-17]. We have analyzed the optical model for increased light extraction from the inside OLED structure by dielectric mirrors, metal mirrors and organic cavity structure [26].
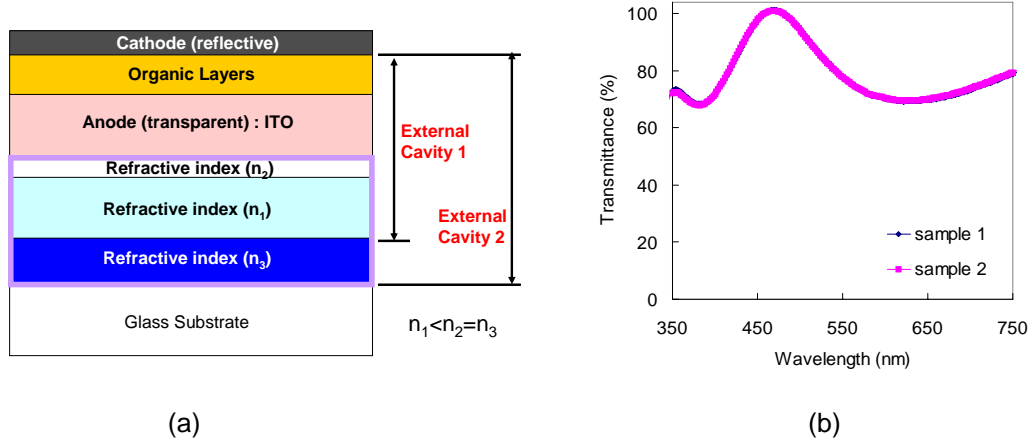

(a)

(b)

Figure 11 (a) Design of non-periodic microcavity structure (b) transmittance of dielectric mirror with structure of TiO$_2$ 54nm /SiO$_2$ 90nm /TiO$_2$ 54nm /Glass

In the present work, we performed numerical and experimental approach to improve the light out-coupling efficiency of conventional bottom-emitting and transparent-type OLED device by use of nanostructured dielectric mirrors (Bragg reflectors). After suitable OLED model was selected, we defined the microcavity structures. The cavity length is expressed by [26-27]

$$L(\lambda) = \frac{\lambda}{2}\left(\frac{n_{eff}}{\Delta n}\right) + \sum_j n_j L_j + \left|\frac{\phi_m}{4\pi}\lambda\right|$$

where n_{eff} and Δn denote the effective refractive index of the DBR and the refractive index difference between SiO$_2$ and TiO$_2$. n_j and L_j are refractive index and thickness of the organic

and indium tin oxide(ITO) layers, respectively. ϕ_m is the phase shift at the metal cathode express by

$$\phi_m = \tan^{-1}\left(\frac{2n_s K_m}{n_s^2 - n_m^2 - k_m^2}\right)$$

where n_s is the refractive index of the organic layer in contact with the metal cathode, and n_m and k_m are the real and imaginary parts of the refractive index of the metal cathode, respectively. Optimum thickness of the cavity is determined using cavity equation. General EL properties and CIE1931 coordinates of microcavity OLED show in Figure 12.
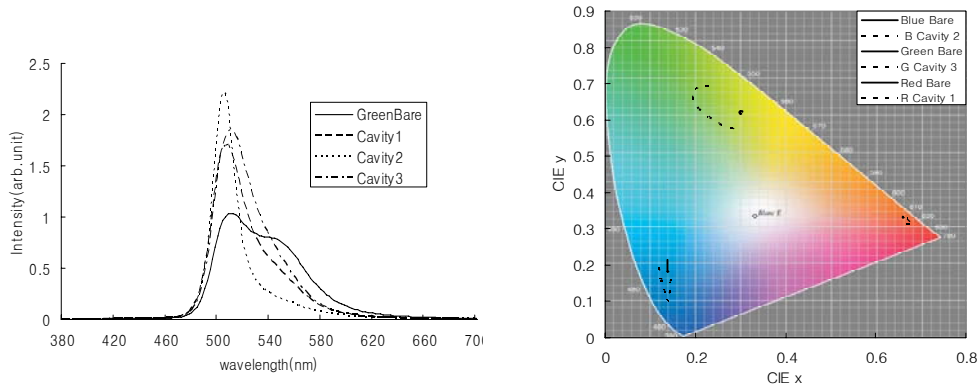

Figure 12. Light emitting spectra of green microcavity-enhanced OLED in comparison to the conventional bottom emission OLED (a) CIE 1931 coordinates of RGB (b) which is simulated at various condition.

All nine Cavity structure show that spectrum intensity increased 30~200% by simulation compared to conventional OLED structure. CIE 1931 coordinates with various angle not seriously changed with such Microcavity structure. Green and blue colors showed improved color purify by the evolution of narrow color spectrum.

Experimentally, the following activities are conducted for enhancing the color gamut and light emitting efficiency of RGB OLEDS with bottom, top-emitting, and transparent design
- Fabrication of nano-structured layers (non-periodic Bragg reflectors)
- Evaluation of OLED device fabrication and further optimization
- Evaluation of the viewing angle characteristics of microcavity-OLED devices
- Combination of nanopatterns (photonic crystal sublayer) and nano-scale Bragg reflectors

Table 3 shows the preliminary experimental results obtained for microcavity OLED using TiO_2/SiO_2 nanostructured sublayers (device structure is ITO/small molecular hole transport material (α-NPB)/fluorescent red host+dopant/electron transport layer (Alq_3)/ LiF/Al). In this condition, red color spectrum was not changed but luminous efficiency was significantly improved by use of microcavity-generating nanoscale layers

Table 3. Effect of microcavity nanoscale layers on red OLED properties

ITO thickness	Microvacity OLED Efficiency *(cd/A)*	Microvacity OLED CIE1931 *(x,y)*	Reference OLED Efficiency *(cd/A)*	Reference OLED CIE1931 *(x,y)*
80nm	8.6 Cd/A	0.665, 0.334	4.3 Cd/A	0.647, 0.352
120nm	6.4 Cd/A	0.662, 0.337	3.6 Cd/A	0.651, 0.348
140nm	4.9 Cd/A	0.665, 0.334	3.4 Cd/A	0.655, 0.344

VI. Potential Application

Top-emitting and transparent OLEDs are originally designed for increased lighting pixel area of active mateix OLED, which enables variety of advanced applications such as thin, light-weight wearable glass and transparent screen. One of OLED's suitable application might be display unit at aircraft, which requires operation at low-pressure condition (Conventional LCD cannot work properly). In spite of many industrial researches and investments on these area, fundamental physics and optical analysison nano-optoelectronic materials for enhanced light extraction is of great importance for next-generation OLED development. Besides the application for thin and transparent display, new broadband white-lighting sources using light, bendable, and transparent substrate are sought to offer significant gains in power efficiency and color quality while having less environmental impact than traditional incandescent and fluorescent lights. Combined with recent progress of organic phosphorescentmaterials, proposed research on nano-patterned OLED structures for improved external luminous efficiency will be essential part of future flat-panel transparent display technology and lighting devices (Figure 13).
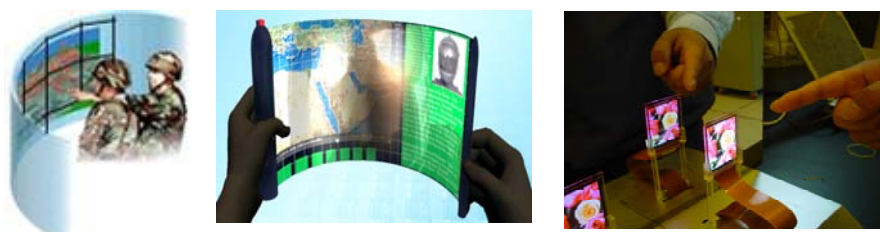
Figure 13. Application of nanostructures for microcavity-enhancing : on the top emission, flexible, or transparent active matrix OLEDs (*Courtesy of USDC/Samsung SDI*)

VII. Plans for Research & Development Activities at 2007

Target and Research Activities (Summary)

Target/Activity	Target/Activity	Methods	% of activity
1. The Efficiency Microcavity-Enhanced OLED	- Red 6.0 cd/A, (0.67, 0.33) - Green 35 cd/A, (0.28, 0.62) - Blue 3.0 cd/A (015, 0.12)	- Novel translucent electrodes - New dielectric layer stack - Optical simulation	30%
2. New Materials for Micro-Lens	- Factor 2.0 increase compared to reference OLED	- Polymeric resin with high-refractive index nanoparticle (composites)	20%
3. Combination of Nanopatterned Layers and Nanostructured layers for planar microcavity	- 30% increase of Target 1 results	- Nanoimprinting for periodic photonic patterns - Effective planarization of OLED pixels	25%
4. Relation with optical device physics and Nanopatterned Layers	- Theoretical study - Correlation with experimental parameters	- Optical simulation - Time of flight mobility measurement - SCLC model - Exciton diffusion and recombination study : Effect of nanostructures on the quantum efficiency enhancement	25%

1. Fabrication of High Efficiency Microcavity-Enhanced OLED

   - Since we have designed the effective microcavity-mode nanostructured layers for various type of OLED device, we would like to optimize the efficiency, brightness, and color spectrum

of such microcavity-enhanced OLED for RGB and white devices

   - Methods for reducing/minimizing angular dependence of light emission, especially for top emitting microcavity devices, will be extensively studied (Figure 14)
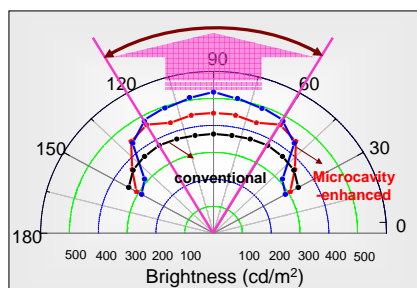

Figure 14. Example of angular dependence of microcavity-enhanced OLEDs

2. New Materials for Micro-Lens

   - Material selection and process for a high-refractive-index material (polymer with inclusion of inorganic particles), which is suitable for cost-effective microlens-processing such as roll-to-roll hot embossing process, will be performed. Details of the pattern size and pitch for enhanced OLED performance will be included for achieving factor of 2.0

3. Combination of Nanopatterned Layers (by imprinting) and Nanoscale Thickness Thin Film Layers for Optimized Microcavity OLED

We will investigate the two-dimensional (2D), periodic, highly ordered array of subwavelength scale of nano-photonic crystal patterns, with a design of architecture, fabrication, and electro-optical characteristics for improved OLEDs. As described by Figure 15, simple nanoimprinting technique will be applied for fabrication of periodic patterns with high-reflective-index materials. This periodic nanostructure will combined with the non-periodic Bragg mirrors for enhanced cavity effect and optical out-coupling enhancement of OLEDs.
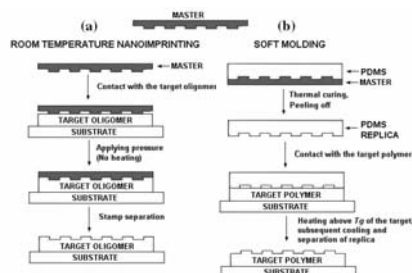

Figure 15. Example of nano (sub-micro) imprinting patterns for substrate/electrode modification of OLEDs
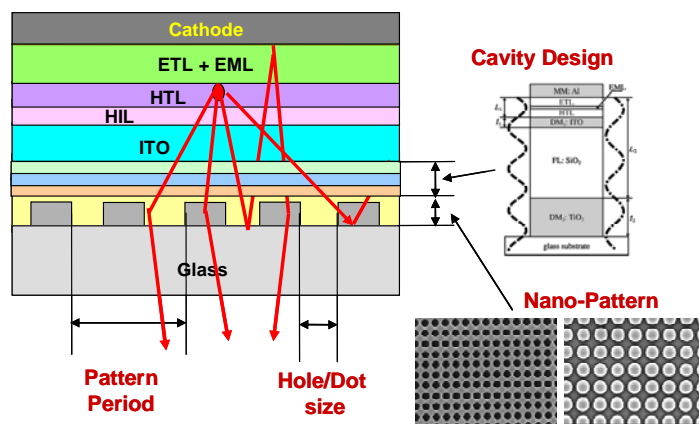
Figure 16. Nanopatterns (imprinted) combined with microcavity design

4. Optimized Top Emission & Transparent OLED

: Enhanced Color reproducibility toward super-RGB and NTSC target

> Red **6 cd/A (0.67, 0.33), Green 35 cd/A (0.28, 0.62), Blue 3 cd/A (0.15, 0.12)**

5. Relation with Optics (Device Physics of Organic Electronic Properties) and Nanopatterned Layers
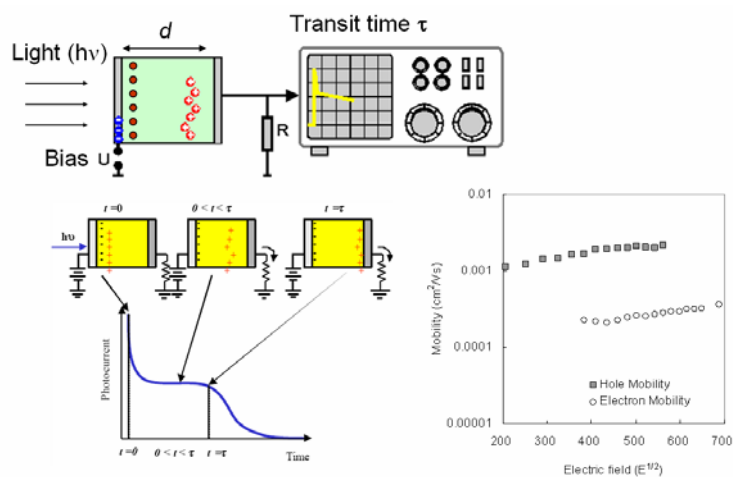

Figure 17. Time of flight (TOF) for measurement of charge carrier mobility

VIII. References

[1] Hung L S, and Chen C H 2002 *Mater. Sci. Eng,* **R39**, 143

[2] Zhou L, Wanga A, Wu S -C, Sun J, Park S and Jackson T N 2006 *Appl. Phys. Lett.* **88,** 083502

[3] Lee J Y, Kwon J H and Chung H K 2003 *Org. Elect.* **4**, 143

[4] Lu M -H, Weaver M S, Zhou T X, Rothman M, Kwong R C, Hack M and Brown J J 2002 *Appl. Phys. Lett.* **81**, 3921

[5] Riel H, Karg S, Beierlein T, Ruhstaller B and Rieß W 2003 *Appl. Phys. Lett.* **82**, 466

[6] Huang Q, Reineke S, Walzer K, Pfeiffer M and Leo K 2006 *Appl. Phys. Lett.* **89**, 263512

[7] Shin H S, Koo J B, Jeong J K, Mo Y G and Chung H K 2005 *Soc. for Information Display (SID) Int Symp. Digest* **36**, 1642

[8] Chen C W, Hsieh P Y, Chiang H H, Lin C L, Wu H M and Wu C C 2003 *Appl. Phys. Lett.* **83,** 5127

[9] Han S, Feng X and Lu Z H 2003 *Appl. Phys. Lett.* **82,** 2715

[10] Pode R B, Lee C J, Moon D G and Han J I 2004 *Appl. Phys. Lett.* **84**, 4614

[11] Wu C C, Lin C -L, Hsieh P -Y and Chiang H -H 2004 *Appl. Phys. Lett.* **84**, 3966

[12] Raychaudhuri P K, Madathil J K, Shore J D and Van Slyke S A, 2004 *J. Soc. Inf. Disp.* **12**, 315

[13] Huang Q, Walzer K, Pfeiffer M, Lyssenko V, He G and Leo K 2006 *Appl. Phys. Lett.* **88**, 113515

[14] Fan, S H, Villeneuve P R, Joannopoulos J D, and Schubert E F 1997 *Phys. Rev. Lett.* **78**, 3294

[15] Schnitzer I, Yablonovitch E, Caneau C, and Gmitter, T J 1993 *Appl. Phys. Lett.* **62**, 131

[16] Moeller S, Forrest S R, *J. Appl. Phys.* 2002 **91**, 3324

[17] So S K, Choi W K, Leung L M, and Neyts K, 1999 *Appl. Phys. Lett.* **74**, 1939

[18] Beierlein T A, Ott H -P, Hofmann H, Riel H, Ruhstaller B, Crone B, Karg S, and Rieß W 2002 *Proc. SPIE* 4464, 178

[19] Bechtel H, Busselt W and Opitz J 2004 *Proc. SPIE* 5519, 194

[20] Riess W, Beierlein T A and Riel H 2004 *Phys. Stat. Sol. (a)* **201**, 1360

[21] Ishibashi T, Yamada J, Hirano R, Iwase Y, Sato Y, Nakagawa R, Sekiya M, Sasaoka T and Urabe T 2006 *Jap. J. Appl. Phys.* **45**, 4392

[22] Suh M C, Chin B D, Kim M H, Kang T M and Lee S T 2003 *Adv. Mater.,* **15**, 1254

[23] Kim M H, Suh M C, Kwon J H, and Chin B D 2007 *Thin Solid Film* **515,** 4011

[24] Lukosz W 1977 *J Opt. Soc. Am.* **67**, 1607

[25] Peng H J, Qiu C F, Xie Z L, Chen H Y, Wong M and Kwok S S 2004 *ASID Symp. Digest* pp.

331-334

[26] Smith L H, Wasey J A E and Barnes W L 2004 *Appl. Phys. Lett.* **84**, 2986

[27] Dodabalapur A, Rothberg L J, Jordan R H, Miller T M, Slusher R E, and Philips J M 2003 *J Appl. Phys* **80** 6954

[28] Fukuda T, Wei B, Ohashi M, Ichikawa M, and Taniguchi Y, 2007 *Jpn. J Appl. Phys* **46**, 642

IX. Journal Papers and Presentation at International Conferences

Journal papers (acknowledged to AFOSR)

1. Byung Doo Chin and Changhee Lee, "Confinement of Charge Carriers and Excitons in the Electrophosphorescent Devices : Mechanism of Light Emission and Degradation" *Advanced Materials*, accepted for publication, (2007)

2. Nam Chul Yang, Jaeho Lee, Myung-Won Song, Nari Ahn, Mu-Hyun Kim, Songtaek Lee, Byung Doo Chin, "Ultra-thin Fluoropolymer Buffer Layer as an Anode Stabilizer of Organic Light Emitting Devices" *J. Phys. D. Appl. Phys.* accepted for publication, (2007)

3. Byung Doo Chin, Nam Su Kang, Jae-Woong Yu, Seong Mu Jo, and Jun Yeob Lee, "Role of interfacial layer on the efficiency and lifetime of polymeric light emitting devices", *Journal of Applied Physics.*, submitted (2007)

4. Byung Doo Chin, "Hybrid Hole Transport Layers for the Color-patterned Top-emitting Organic Light Emitting Devices", *J. Phys. D. Appl. Phys.*, submitted (2007)

International Conferences

1. Byung Doo Chin, Jai Kyeong Kim, "Microcavity-enhanced White OLED for efficient lighting application", *International Meeting on Information Display (IMID 2006)* Taegu, August 25, 2006.

2. Byung Doo Chin, Soo-Hyeong Lee, Jai Kyeong Kim, Chang Hee Lee, "Role of carrier mobility, exciton diffusion, and their interplay for charge balance and improved properties of organic electrophosphorescent device", *SPIE Optics and Photonics,* 13 - 17 August 2006, San Diego, California, USA (Proceedings of SPIE Volume **6333 -** Organic Light Emitting Materials and Devices X)

3. Byung Doo Chin, Jai Kyeong Kim, O Ok Park, "Efficient white OLED for lighting application: combination of fluorescent and phosphorescent light emitting materials" *ICSM (International conference on Science and Technology of Synthetic Metals) 2006*, July 5. Dublin, Ireland

X. Participated Investigators and Budget Table

1. Participated Investigators

Dr. Byung Doo Chin, KIST

  - Design, fabrication, and investigation of top emitting and transparent OLED

Dr. Jai Kyeong Kim, KIST

  - Micro-lens array

Mr. N. S. Kang, KIST

  - Experimental works for transparent electrode fabrication, organic layer deposition

  - Design of optical microcavity array

  - Nanostructured layer fabrication for OLED

Mr. H. K. Lee

  - Experimental works for organic phosphorescent devices

Mr. Y. H. Lee

  - Experimental works for white OLED devices

2. Budget ×1,000 Korean won

	Titles		2006 Budget	2006 Consumed	etc.
1	Salaries		25,000	25,000	
2	Overheads	Overhead Charges	20,000	20,000	
		Sub-total	45,000	45,000	
3	Salaries (for students)		13,000	13,000	
4	Direct Costs	Travel Expenses	5,500	5,500	
		Fees for purchasing technical Information	3,750	3,750	
		Equipments	9,500	9,500	
		Consumable Materials	17,000	17,000	
		Demonstrating setup			
		Miscellaneous	2,500 3,750	2,500 3,750	
		Sub-total	42,000	42,000	
5	Sub-project				
	Total		100,000	100,000	

May. 9th 2007, Prepared by BDC